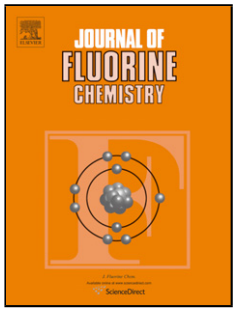

Title: A methodology for the photocatalyzed radical trifluoromethylation of indoles: a combined experimental and computational study

Authors: Shelli A. Miller, Bas van Beek, Trevor A. Hamlin, F. Matthias Bickelhaupt, Nicholas E. Leadbeater

PII: S0022-1139(18)30283-5
DOI: https://doi.org/10.1016/j.jfluchem.2018.08.005
Reference: FLUOR 9209

To appear in: *FLUOR*

Received date: 11-7-2018
Revised date: 9-8-2018
Accepted date: 9-8-2018

Please cite this article as: Miller SA, van Beek B, Hamlin TA, Bickelhaupt FM, Leadbeater NE, A methodology for the photocatalyzed radical trifluoromethylation of indoles: a combined experimental and computational study, *Journal of Fluorine Chemistry* (2018), https://doi.org/10.1016/j.jfluchem.2018.08.005

A methodology for the photocatalyzed radical trifluoromethylation of indoles: a combined experimental and computational study

Shelli A. Miller,[a] Bas van Beek,[b] Trevor A. Hamlin,*[b] F. Matthias Bickelhaupt,[b,c] and Nicholas E. Leadbeater*[a]

[a] *Department of Chemistry, University of Connecticut, 55 North Eagleville Road, Storrs, Connecticut 06269-3060, United States*

[b] *Department of Theoretical Chemistry and Amsterdam Center for Multiscale Modeling (ACMM), Vrije Universiteit Amsterdam, De Boelelaan 1083, NL-1081 HV Amsterdam, The Netherlands*

[c] *Institute for Molecules and Materials (IMM), Radboud University, Heyendaalseweg 135, NL-6525 AJ Nijmegen, The Netherlands*

Graphical Abstract

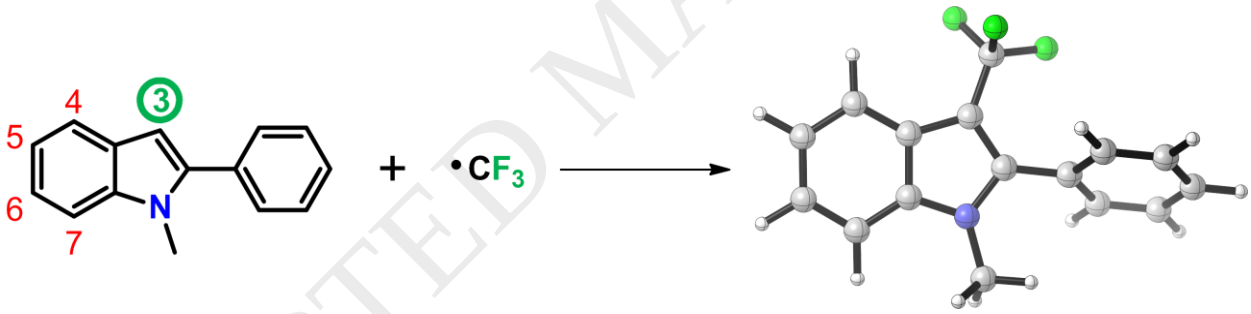

HIGHLIGHTS

- A methodology for the direct introduction of the trifluoromethyl group on to indole scaffolds is presented.
- Sodium trifluoromethylsulfinate (Langlois reagent) is used as the source of the trifluoromethyl radical
- Reactions are performed photochemically with 2-*t*butylanthraquinone as a photocatalyst.

- Quantum chemical computations successfully predict and rationalize the formation of the experimentally observed products.

ABSTRACT

A methodology for the direct introduction of the trifluoromethyl group on to indole scaffolds is presented. The procedure involves the use of sodium trifluoromethylsulfinate (Langlois reagent) as the source of the trifluoromethyl radical, and is performed photochemically with 2-*tert*-butylanthraquinone as a photocatalyst. The reaction has also been probed computationally. Reaction kinetics and molecular orbital analyses from our quantum chemical computations successfully predict and rationalize the formation of the experimentally observed product and, in the case of 1-methylbenzimidazole, even reproduce the same qualitative trends in regioisomer preference.

KEYWORDS

Photocatalysis, Trifluoromethylation, Langlois reagent, Indoles, Density functional calculations

1. INTRODUCTION

The incorporation of fluorine atoms or fluorine-containing groups into organic molecules is a current topic of considerable interest both in academic and industrial settings.[1,2] As a result, synthetic strategies which achieve fluorination are desirable based on the properties conferred to the fluorinated product.[3] For example, carbon-fluorine bonds are not only stronger than analogous C-H bonds, but are also more polarized, making them more resistant against oxidative metabolism.[4] While monofluoro- and difluoro-moieties are certainly of interest, the trifluoromethyl functionality (-CF_3) has received significant attention, likely because of its ability to serve as a bioisostere for several functional groups.[5] This bioisosteric property can be used to adjust the steric and electronic properties of a compound, or to prevent metabolic degradation.[6] A range of synthetic strategies are available for performing trifluoromethylation reactions,[7] examples being the use of the Umemoto,[8] Togni,[9] Langlois,[10] and Rupert-Prakash[11] reagents (Figure 1).

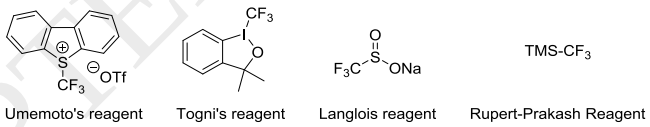

Figure 1. Structures of common trifluoromethylating reagents

One approach to the direct trifluoromethylation of substrates involves the use of trifluoromethyl radical sources.[12] Other methods of trifluoromethylating, such as cross-coupling reactions, are at a disadvantage to direct radical methods because they require pre-functionalized substrates, while direct radical methods do not. In the realm of radical trifluoromethylation reactions, the Langlois reagent has proven particularly popular, being

a relatively inexpensive, bench stable solid. It has garnered much attention since Baran and co-workers reported its application in an efficient methodology for the trifluoromethylation of heterocycles in 2011 (Figure 2).[13] Since then, a number of peroxide-free methods have been proposed. These generally rely on the use of either transition metals, inert atmosphere, harsh conditions, or combination thereof.[14-17]

In hopes of developing an efficient and mild approach to radical trifluoromethylation, some have been turning to the use of photocatalysis. The popularity of photocatalysis as a tool in preparative organic chemistry has been growing exponentially in recent years.[18] These methods have opened avenues to chemical transformations that are otherwise unachievable. Photochemical approaches to radical trifluoromethylation using the Langlois reagent have been reported, but they tend to require rigorously anhydrous and anaerobic conditions, as well as the use of transition metals (Figure 3).[18-21] Nicewicz found that the Langlois reagent could be used, in conjunction with an organic acridinium based photocatalyst, to facilitate the hydrotrifluoromethylation of alkenes, resulting in 25-74% yields.[21] This method, using blue LED light (λ = 450 nm), requires stoichiometric amounts of methyl thiosalicylate or thiophenol, which act as hydrogen atom donors. Similarly, Lefebvre later reported a hydrotrifluoromethylation method which explored the reactivity of electron-deficient substrates.[20] They employ a benzophenone-based photocatalyst in conjunction with UV light (λ = 355 nm) and use hexafluoroisopropanol (HFIP) as a super-stoichiometric additive, lending some credence to previous observations that HFIP can act as a proton donor rather than a hydrogen atom donor. They also demonstrate that similar yields can be obtained when employing an iridium-based photocatalyst and blue light. Itoh and co-workers have reported the use of an anthraquinone derivative as an organic

photocatalyst for the trifluoromethylation of arenes and heteroarenes, however, this method still requires an inert atmosphere, and has a limited substrate scope.[19] Interestingly, when there is more than one reactive site, a degree of regioselectivity is observed in electron-rich arenes.

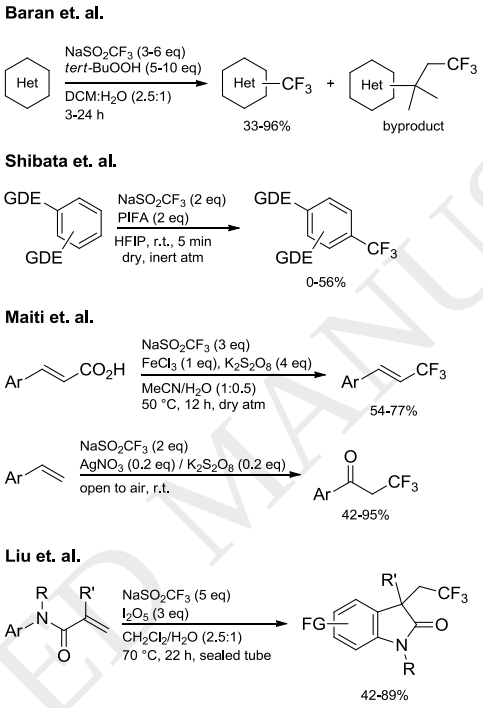

Figure 2. Examples of the use of the Langlois reagent in trifluoromethylation reactions

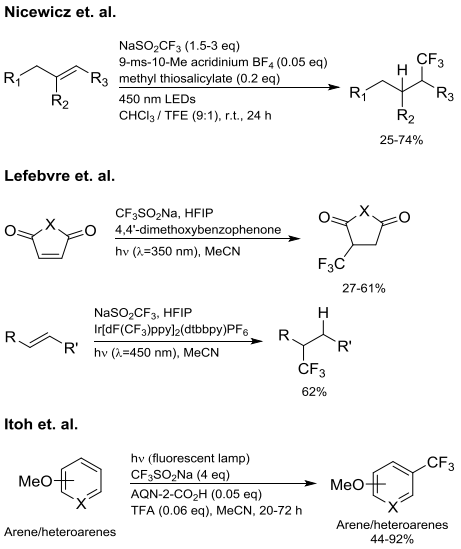

Figure 3. Examples of the use of the Langlois reagent in photo-mediated trifluoromethylation reactions

Unrelated to organofluorine chemistry, the Itoh group have recently reported a methodology for the visible-light mediated cross-dehydrogenative C-H amination of indoles with phthalimides, employing 2-*tert*-butylanthraquinone as a photocatalyst (Figure 4).[23] Having already developed a number of non-radical approaches to trifluoromethylation,[24] the reports by Itoh piqued our interest and we sought to develop a methodology for the photo-mediated radical trifluoromethylation of indoles using Langlois reagent and an anthraquinone photocatalyst. Incorporation of fluorine into indole scaffolds is very attractive due to the prevalence of indoles in natural products and pharmaceuticals. Photo-mediated trifluoromethylation of indoles has been the subject of previous studies, although not using Langlois reagent (Figure 5).[25] We wanted to expand on these previous reports, offering an additional approach for the synthesis of these valuable products. Our metal-free method is convenient in that rigorously anhydrous and / or anaerobic conditions are not required. While product yields are moderate, they are not unlike many of the other methods

reported in the literature. To augment our synthetic chemistry, we employed computational chemistry to help us understand why yields for 2- or 3-substituted trifluoromethylated indoles can be quite low.

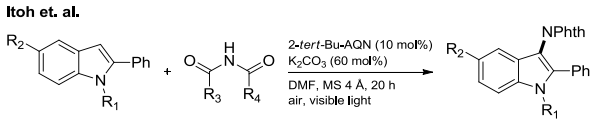

Figure 4. The visible-light mediated cross-dehydrogenative C-H amination of indoles

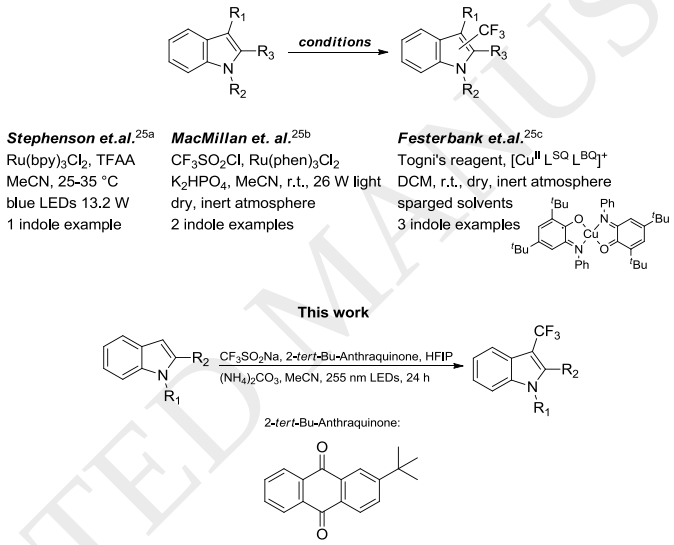

Figure 5. Key previous methods for photo-mediated trifluoromethylation of indoles, and our approach

2. RESULTS AND DISCUSSION

As a substrate for reaction optimization, we selected 1-methyl-2-phenylindole (**1a**). Employing DMF as our solvent (0.1 M in substrate), 1 eq of Langlois reagent, 0.6 eq of potassium carbonate as a base, 10 mol% 2-*tert*-butylanthraquinone (AQN) as a photocatalyst, and a blue LED light source, we obtained a 10 % yield by NMR of the desired

trifluoromethylated product after 24 h (Table 1, entry 1). The reaction was performed in a sealed Pyrex test tube using approximately 50 mg of 4 Å molecular sieves to sequester water. The λ-max of AQN is 255 nm, and keeping all parameters constant with the exception of switching the light source to 255 nm LEDs and using a quartz reaction tube increased the yield to 32% (entry 2). Changing the photocatalyst to 9-mesityl-10-methyl acridinium tetrafluoroborate and using blue light, a 10% yield was obtained, suggesting that AQN was superior (entry 3). Doubling both the photocatalyst loading and also the quantity of Langlois reagent increased the yield to 47% (entry 4). Changing the solvent to acetonitrile not only increased the product yield to 50%, but also dramatically decreased the necessary reaction time to 3 h (entry 5). Cesium carbonate and ammonium carbonate were screened as alternative bases and both found to be on par with potassium carbonate (entries 6 and 7). Thus, we decided to proceed using ammonium carbonate due to its increased solubility in acetonitrile, thereby allowing for the more effective stirring of the reaction mixture. Performing the reaction either open to the atmosphere or under a balloon of air slightly increased product conversion, but at the expense of increasing reaction time (entries 8 and 9). An atmosphere of nitrogen doubled the reaction time with no effect on yield (entry 10). Under an oxygen atmosphere, the reaction was greatly accelerated at the expense of the desired product (entry 11), a number of side products being formed. While these were not identified, they are believed to be polymeric in nature and if the reaction is left for longer, decomposition occurs. To avoid loss of solvent due to evaporation and the formation of these undesired side products, we decided to proceed using a balloon of air. Knowing that HFIP can play a profound effect on reaction rate and outcome,[26] we performed two trials with the addition of 0.5 eq and 0.25 eq of HFIP to the reaction mixture. Using 0.5 eq HFIP increased

the yield to 57% after 48 h (entry 12), but when reduced to 0.25 eq HFIP we obtained a 61% yield after just 24 h (entry 13). These conditions were taken on to the substrate screen. Three negative control experiments were also run to confirm that all components of the reaction mixture were necessary. The reaction did not occur in the absence of light, photocatalyst, or base (entries 14-16). In addition, performing the reaction under an atmosphere of nitrogen along with the addition of HFIP did not have a discernable effect on the outcome of the reaction (entry 17).

Table 1. Optimization of reaction conditions[a]

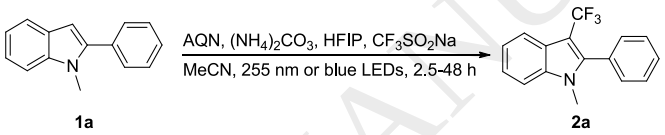

1a **2a**

Entry	Solvent	Catalyst (mol%)	Base	CF_3SO_2Na (eq)	Additive (eq)	Light	Atm	Time (h)	Yield (%)
1	DMF	AQN (10)	K_2CO_3	1	-	blue	Closed	20	10
2	DMF	AQN (10)	K_2CO_3	1	-	255	Closed	20	32
3	DMF	9-Ms-10-MeAcr (10)	K_2CO_3	1	-	blue	Closed	20	10
4	DMF	AQN (20)	K_2CO_3	2	-	255	Closed	20	47
5	MeCN	AQN (20)	K_2CO_3	2	-	255	Closed	3	50
6	MeCN	AQN (20)	Cs_2CO_3	2	-	255	Closed	3	46
7	MeCN	AQN (20)	$(NH_4)_2CO_3$	2	-	255	Closed	3	50
8	MeCN	AQN (20)	$(NH_4)_2CO_3$	2	-	255	Open	9	57
9	MeCN	AQN (20)	$(NH_4)_2CO_3$	3	-	255	Lab air	8	55
10	MeCN	AQN (20)	$(NH_4)_2CO_3$	3	-	255	N_2	48	57
11	MeCN	AQN (20)	$(NH_4)_2CO_3$	3	-	255	O_2	2.5	37
12	MeCN	AQN (20)	$(NH_4)_2CO_3$	2	HFIP (0.5)	255	Lab air	48	57
13	**MeCN**	**AQN (20)**	**$(NH_4)_2CO_3$**	**2**	**HFIP (0.25)**	**255**	**Lab air**	**24**	**61**
14	MeCN	-	$(NH_4)_2CO_3$	2	HFIP (0.25)	255	Lab air	24	*no product*
15	MeCN	AQN (20)	-	2	HFIP (0.25)	255	Lab air	24	*no product*
16	MeCN	AQN (20)	$(NH_4)_2CO_3$	2	HFIP (0.25)	-	Lab air	24	*no product*
17	MeCN	AQN (20)	$(NH_4)_2CO_3$	3	HFIP (0.5)	255	N_2	48	54

[a] Reactions were performed on the 0.3 mmol scale at a concentration of 0.1 M, using 0.6 eq base. They were monitored by TLC and worked up after the disappearance of the starting material. [b] Yield by quantitative ^{1}H NMR.

We began our substrate scope using 2-substituted indoles as reagents (Table 2). We determined product yields initially using quantitative NMR spectroscopy on the crude product mixture and then isolating the products using preparative thin-layer

chromatography. Substrates that were not *N*-methyl-substituted were found to have similar reactivity to their *N*-methyl-substituted analogues (Table 2, entries 1-3). The substituent at the 2-position was varied. Placing a methyl group at the 2-position led to lower conversions (entries 4 and 5). One other nitrogen protecting group, MOM, was found to be comparable to the *N*-methyl protected analogue (entry 6). Unfortunately, when trying to expand the scope to non-nitrogen containing systems, we found benzofurans and the more biologically active uracil were unreactive (entries 7 and 8).

Table 2. Substrate screening of 2-substituted indoles

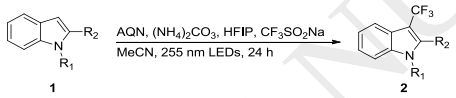

1 2

Entry	Product	Yield[b] (%)
1	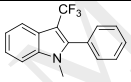 **2a**	46 (61)
2	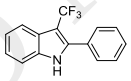 **2b**	47 (67)
3	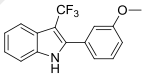 **2c**	30 (61)
4	 **2d**	16 (33)
5	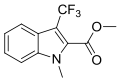 **2e**	30 (48)
6	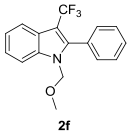 **2f**	38 (46)
7	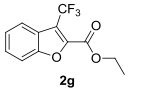 **2g**	N.R.
8	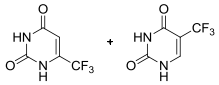 **2h** + **2h'**	N.R.

[a] Indole (0.3 mmol, 1 eq), sodium trifluoromethylsulfinate (0.6 mmol, 2 eq), 2-*tert*-butyl anthraquinone (0.06 mmol, 0.2 eq), ammonium carbonate (0.18 mmol, 0.6 eq), HFIP (0.075 mmol, 0.25 eq), and acetonitrile (3 mL, 0.1 M) in a sealed quartz tube with a balloon of air and irradiated at 255 nm for 24 h. N.R. = no reaction. [b] Isolated yields; values in parentheses are yields obtained using quantitative ^{1}H-NMR spectroscopy.

When using 3-substituted indoles as substrates, product conversions were lower than in the case of the 2-substituted analogues (Table 3). The formation of multiple unidentified side products and decomposition was observed, thus making for a challenging isolation of the desired product. In the case of unsubstituted indoles, both 2- and 3-trifluoromethylated products were formed, this not being unexpected (Table 4). In light of the range of side products formed in some of these reactions, we decided to screen 1-methylbenzimidazole as a substrate and we again obtained a range of trifluoromethylated products, but in this case, we characterized and isolated each of them (Table 5).

Table 3. Substrate screening of 3-substituted indoles

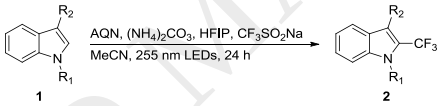

1 2

Entry	Product	Yield[b] (%)
1	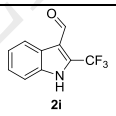 **2i**	3 (10)
2	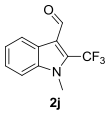 **2j**	(5)
3	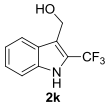 **2k**	25 (39)

[a] Indole (0.3 mmol, 1 eq), sodium trifluoromethylsulfinate (0.6 mmol, 2 eq), 2-*tert*-butyl anthraquinone (0.06 mmol, 0.2 eq), ammonium carbonate (0.18 mmol, 0.6 eq), HFIP (0.075 mmol, 0.25 eq), and acetonitrile (3 mL, 0.1 M) in a sealed quartz tube with a balloon of air and irradiated at 255 nm for 24 h. [b] Isolated yields; values in parentheses are yields obtained using quantitative ^{1}H-NMR spectroscopy.

Table 4. Substrate screening of unsubstituted indoles

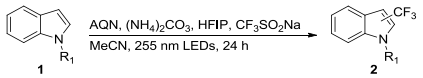

Entry	Product	Yield[b] (%)
1	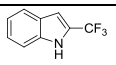 2l	(12)
2	 2l'	(26)
3	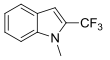 2m	(4)
4	 2m'	(5)

[a] Indole (0.3 mmol, 1 eq), sodium trifluoromethylsulfinate (0.6 mmol, 2 eq), 2-*tert*-butyl anthraquinone (0.06 mmol, 0.2 eq), ammonium carbonate (0.18 mmol, 0.6 eq), HFIP (0.075 mmol, 0.25 eq), and acetonitrile (3 mL, 0.1 M) in a sealed quartz tube with a balloon of air and irradiated at 255 nm for 24 h. [b] Values in parentheses are yields obtained using quantitative ^{1}H-NMR spectroscopy

Table 5. Product distribution obtained in the reaction of 1-methylbenzimidazole (**3**)

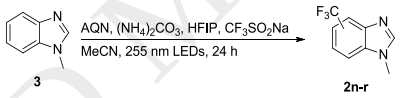

Entry	Product	Yield[b] (%)
1	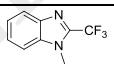 2n	7
2	 2o	19
3	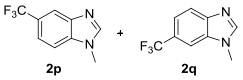 2p 2q	6 (1:1 ratio)
4	 2r	3

[a] 1-Methylbenzimidazole (0.3 mmol, 1 eq), sodium trifluoromethylsulfinate (0.6 mmol, 2 eq), 2-*tert*-butyl anthraquinone (0.06 mmol, 0.2 eq), ammonium carbonate (0.18 mmol, 0.6 eq), HFIP (0.075 mmol, 0.25 eq), and acetonitrile (3 mL, 0.1 M) in a sealed quartz tube with a balloon of air and irradiated at 255 nm for 24 h. [b] Isolated yields.

In order to probe the reaction in more detail, the regioselectivity of the aromatic CF_3 radical addition was evaluated using DFT calculations at the (U)BP86/TZ2P level[27-

[29] with the ADF program.[30,31] Acetonitrile (ε = 37.5) was simulated in all optimizations using the COSMO solvation model.[32-35] Gibbs free energies (ΔG) account for zero-point and thermal energy, changes in volume and pressure, and entropy effects at 298.15 K and 1 atm. The regioselectivity of the trifluoromethylation of 1-methyl-2-phenyl indole (**1a**) and 1-methylbenzimidazole (**3**) have been evaluated, as the former serves as a good model system with a common core structure and the latter has all other identified minor products fully characterized (Table 5).

The potential energy surface was calculated based on the generally accepted model of the photochemical generation of the CF_3 radical (**4**) and subsequent addition to the indole (**1a**) or benzimidazole (**3**). This approach is in line with the method proposed by Houk and co-workers, which assumes that the energy associated with the aromatic CF_3 radical adduct (**2.IC**) is an adequate approximation to the energy of the actual transition state (Figure 6).[36] The low experimentally and computationally determined barriers reported for CF_3 radical additions motivate the use of this approach.[37-40] Barriers are expected to be further lowered due to the stabilizing influence of the aromatic rings.[41]

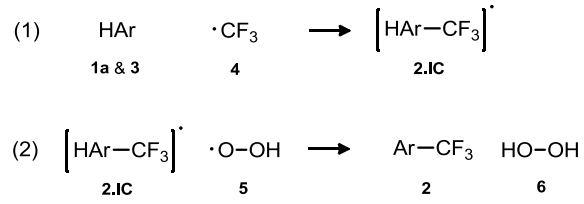

Figure 6. Reaction scheme for CF_3 functionalization. HAr = 1-methy-2-phenylindole (**1a**) or 1-methylbenzimidazole (**3**)

The Gibbs free energies (ΔG_{IC} – intermediate complex, ΔG_P – products) associated with trifluoromethyl radical addition to compounds **1a** and **3** are shown in Table 6. These substrates are primarily trifluoromethylated at C_3 and C_4, respectively, and analysis of the ΔG_{IC} values reveals that radical addition at those positions is preferred compared to the other possible sites. The reaction energy (ΔG_P) does not correlate with the experimentally observed major product, thus these reactions likely operate under kinetic control. The low barrier for CF_3 radical addition leads to the intermediate complex (IC), which is then rapidly quenched via a highly exergonic reaction leading to the product (P). Interestingly, CF_3 radical addition to **1a** at C_3 has a very small $\Delta\Delta G_{IC}$ value (ca 0.3 kcal mol^{-1}), possibly explaining the poor yields.

Table 6: Computed reaction energies[a] for the stationary points of **1a** and **3** [intermediate complexes (IC) and products (P)]. Energetically preferred pathways are highlighted in bold

Position:		2	3	4	5	6	7
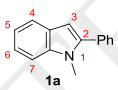 **1a**	IC	-	**–8.9**	–8.6	–2.2	–5.9	–3.1
	P	-	–60.4	–61.7	**–63.8**	–61.8	–55.9
 **3**	IC	–14.8	-	**–16.6**	–11.6	–13.7	–12.7
	P	–65.3	-	–70.8	**–72.3**	–71.9	–66.9

[a] Gibbs free energies (kcal mol^{-1}, 298.15 K, 1 atm) computed at the COSMO(MeCN)-(U)BP86/TZ2P level

Focusing on the analysis of compound **3**, for which we have experimentally identified and quantified all possible regioisomers, the same general trends in regioselectivity are observed as initially shown for **1a**. The ΔG_{IC} energies correctly rationalize the same

qualitative trends in regioselectivity. Nevertheless, while the computations reproduce the correct trend, a systematic overestimation of the regioselectivity is observed (Table 7), *i.e.* the computed values of $\Delta\Delta G_{IC}$ are consistently too large. This may be the result of neglecting the TS associated with CF_3 radical addition, with a $\Delta\Delta G_{TS}$ of merely 0.5 kcal mol^{-1} being sufficient to reproduce the observed ratio between positions 4 and 7.

Table 7: Experimental (Exp.) and computed (Comp.) product ratios. Computed ratios based on $\Delta\Delta G_{IC}$.

Position:	2	4	5	6	7
Exp.	0.20	0.54	0.17[a]		0.09
Comp.	0.06	0.93	0.00	0.01	0.00

[a] Combination of regioisomer **5** and **6**

Next, we rationalized the preference for the observed reaction sites based on a frontier molecular orbital (FMO) analysis. The key FMO interaction is a two-center/three-electron bond between the $HOMO_{\mathbf{1a,3}}$ and $SOMO_{CF3}$, with calculated energy gaps of 1.7 and 1.1 eV for the IC of **1** and **3a**, respectively (Figure 7). The other FMO interaction, between the $SOMO_{CF3}$ and $LUMO_{\mathbf{1a,3}}$, is weaker with larger energy gaps (**1a** – 4.0 eV; **3** – 4.0 eV). The small $HOMO_{\mathbf{1a,3}}$–$SOMO_{CF3}$ gap, combined with a favorable orbital overlap (**1a** – 0.29; **3** – 0.27), emphasizes the established electrophilic nature of the CF_3 radical and the primary role of the $SOMO_{CF3}$ as an electron-acceptor, rather than donor.[42] Additionally, we found that the carbon with the largest $HOMO_{\mathbf{1a,3}}$ coefficient is also the one that leads to the kinetically favorable IC (Figure 8, **1a** – C_3, **3** – C_4). This evidence highlights the key FMO interactions underpinning the observed reactivity of the indoles in this radical addition reaction.

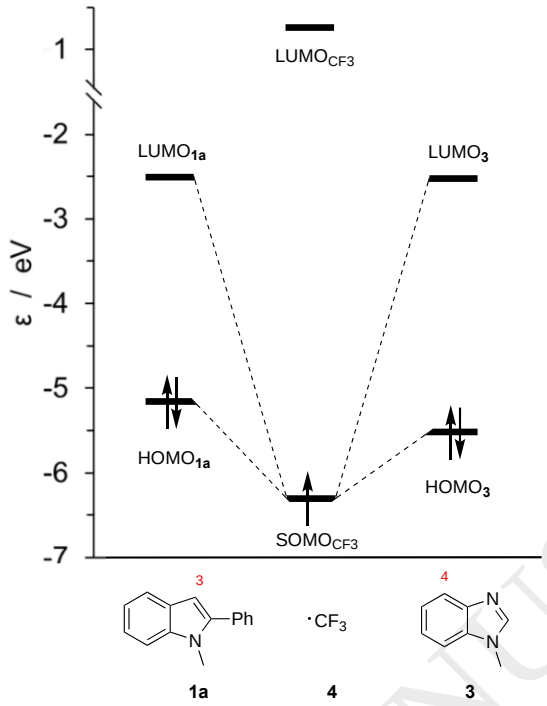

	De HOMO$_{1a,3}$–SOMO$_{CF3}$ (eV)	Orbital Overlap (S)
1a	1.7	0.29
3	1.1	0.27

	De SOMO$_{CF3}$LUMO$_{1a,3}$ (eV)	Orbital Overlap (S)
1a	4.0	0.17
3	4.0	0.23

Figure 7. Indole/benzimidazole (**1a** and **3**) and CF_3 (**4**) frontier molecular orbital (FMO) gaps and overlaps of the kinetically most favorable intermediate complexes (C_3 and C_4, respectively). FMO overlap and energy gaps are based on restricted open-shell molecular fragments

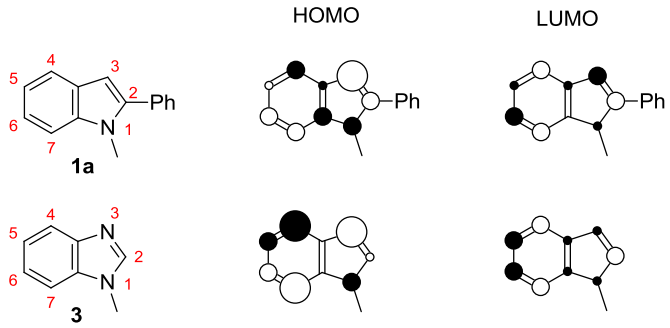

Figure 8: Qualitative representation of the HOMO$_{1a,3}$ and LUMO$_{1a,3}$ based on MO coefficients calculated at the COSMO(MeCN)-(U)BP86/TZ2P level

CONCLUSION

We have developed a methodology for the direct introduction of the trifluoromethyl group on to indole scaffolds. The procedure involves the use of sodium trifluoromethylsulfinate (Langlois reagent) as the source of the trifluoromethyl radical and is performed photochemically with 2-*tert*-butylanthraquinone as a photocatalyst. We have also probed the reaction computationally. Our computed reaction kinetics successfully predict the formation of the experimentally observed product and, in the case of 1-methylbenzimidazole, even reproduce the same qualitative trends in regioisomer preference. This regioselectivity was rationalized by means of an orbital analysis, which highlighted the key $HOMO_{\mathbf{1a},3}|SOMO_{CF3}$ interaction due to its small energy gap and favorable overlap. Additionally, we discovered that the carbon associated with the kinetically most favorable site consistently has the largest contribution to the $HOMO_{\mathbf{1a},3}$. This orbital analysis serves as an affordable method to predict the experimental regioselectivity of this trifluoromethyl radical addition reaction.

4. EXPERIMENTAL SECTION

4.1. Determination of product conversion using quantitative NMR spectroscopy

NMR Spectra (^{1}H, ^{13}C, ^{19}F) were performed at 298 K on a Brüker Avance III nanobay 400 MHz NMR spectrometer equipped with 5 mm BBFO probe. ^{1}H-NMR Spectra obtained in $CDCl_3$ were referenced to residual non-deuterated chloroform (7.26 ppm) in the deuterated solvent. ^{13}C-NMR Spectra obtained in $CDCl_3$ were referenced to chloroform (77.2 ppm). ^{19}F-NMR spectra were referenced to hexafluorobenzene (–162.4 ppm). Product conversions determined using quantitative NMR spectroscopy were obtained via the *ERETIC* method

(*E*lectronic *RE*ference *T*o access *I*n-vivo *C*oncentrations)[43] in Brüker TopSpin 3.5 and calculated using 1,2,4,5-tetramethylbenzene (83.44 mM) as an external standard, with a P1 value of 15.62 microseconds and D1 value of 5 s.

4.2. General procedure for the preparation of trifluoromethyl-substituted indoles: The desired indole (0.3 mmol, 1 eq) was mixed with sodium trifluoromethylsulfinate (0.6 mmol, 2 eq), 2-*tert*-butylanthraquinone (0.06 mmol, 0.2 eq), ammonium carbonate (0.18 mmol, 0.6 eq), hexafluoroisopropyl alcohol (0.075 mmol, 0.25 eq), and acetonitrile (3 mL, 0.1 M) in a sealed quartz tube with a balloon of air and irradiated at 255 nm for 24 h. The reaction was quenched with water and extracted with dichloromethane or EtOAc (3 x 30 mL). The combined organic layers were dried over sodium sulfate, filtered, and the solvent removed *in vacuo*. The desired product was then isolated using preparative TLC with the appropriate solvent system.

*1-Methyl-2-phenyl-3-(trifluoromethyl)-1H-indole (**2a**)*[17] was purified using 95:5 Hex:EtOAc to give a yellow solid (38 mg, 46%). **^{1}H NMR** (400 MHz, $CDCl_3$) δ ppm 7.88-7.78 (dd, 1H), 7.55-7.47 (m, 3H), 7.45-7.37 (m, 3H), 7.34 (m, 1H), 7.27 (td, *J* = 7.5, 7.0, 1.2 Hz, 1H), 3.54 (s, 3H). **^{13}C NMR** (100 MHz, $CDCl_3$, 100 MHz) δ ppm 140.9 (q, *J* = 4.0 Hz), 136.5, 130.6 (q, *J* = 1.2 Hz), 130.3, 129.5, 128.5, 124.9 (q, *J* = 267.2 Hz), 124.6 (q, *J* = 1.8 Hz), 123.1, 121.7, 120.0 (q, *J* = 1.5 Hz), 110.1, 104.2 (q, J = 35.2 Hz), 30.9. **^{19}F NMR** (376 MHz, $CDCl_3$) δ ppm -53.39.

5. ACKNOWLEDGEMENTS

This work was supported financially by the University of Connecticut. Additionally, we thank the Netherlands Organization for Scientific Research (NWO) for financial support through

the Planetary and Exo-Planetary Science program (PEPSci) and the Dutch Astrochemistry Network (DAN). We would also like to thank undergraduate students Joshua Paolillo and Madeline Williams (University of Connecticut) for contributions to the experimental components of this project.

6. SUPPORTING INFORMATION

Experimental and computational details, ^{1}H, ^{13}C, and ^{19}F NMR spectra of the compounds prepared.

REFERENCES

1. A. Harsanyi, G. Sandford, Green Chem. 17 (2015) 2081-2086.
2. (a) W. K. Hagmann, J. Med. Chem. 51 (2008) 4359-4369. (b) D. O'Hagan, Chem. Soc. Rev. 37 (2008) 308-319.
3. (a) T. Liang, C. N. Neumann, T. Ritter, Angew. Chem. Int. Ed. 52 (2013) 8214-8264; (b) H. Vorbrueggen, Helv. Chim. Acta 94 (2011) 947-965; (c) K. Müller, C. Faeh, F. Diederich, Science 317 (2007) 1881-1886.
4. (a) R. R. Frey, C. K. Wada, R. B. Garland, M. L. Curtin, M. R. Michaelides, J. Li, L. J. Pease, K. B. Glaser, P. A. Marcotte, J. J. Bouska, S. S. Murphy, S. K. Davidsen, Bioorg. Med. Chem. Lett. 12 (2002) 3443-3447; (b) A. S. Madsen, C. A. Olsen, Med. Chem. Commun. 7 (2016) 464-470.
5. (a) N. A. Meanwell, J. Med. Chem. [Online early access]. DOI: 10.1021/acs.jmedchem.7b01788. Published Online: February 5, 2018. https://pubs.acs.org/doi/abs/10.1021%2Facs.jmedchem.7b01788 (accessed July 6, 2018). (b) I. G. Molnár, C. Thiehoff, M. C. Holland, R. Gilmour, ACS Catal. 6 (2016) 7167-7173; (c) N. A. Meanwell, J. Med. Chem. 54 (2011) 54, 2529-2591.
6. M. Jagodzinska, F. Huguenot, G. Candiani, M. Zanda, ChemMedChem 4 (2009) 49-51.
7. S. Barata-Vallejo, B. Lantaño, A. Postigo, Chem. Eur. J. 20 (2014) 16806-16829.
8. T. Umemoto, S. Ishihara, Tetrahedron Lett. 31 (1990) 3579-3582.
9. P. Eisenberger, S. Gischig, A. Togni, Chem. Eur. J. 12 (2006) 2579-2586.
10. B. R. Langlois, E. Laurent, N. Roidot, Tetrahedron Lett. 32 (1991) 7525-7528.

11. (a) R. Krishnamurti, D. R. Bellew, G. K. S. Prakash, J. Org. Chem. 56 (1991) 984-989. (b) I. Ruppert, K. Schlich, W. Volbach, Tetrahedron Lett. 25 (1984) 2195-2198.

12. A. Studer, Angew. Chem. Int. Ed. 51 (2012) 8950-8958.

13. Y. Ji, T. Brueckl, R. D. Baxter, Y. Fujiwara, I. B. Seiple, S. Su, D. G. Blackmond, P. S. Baran, Proc. Natl. Acad. Sci. U.S.A. 108 (2011) 14411-14415.

14. A. Deb, S. Manna, A. Modak, T. Patra, S. Maity, D. Maiti, Angew. Chem. Int. Ed. 52 (2013) 9747-9750.

15. T. Patra, A. Deb, S. Manna, U. Sharma, D. Maiti, Eur. J. Org. Chem. (2013) 5247-5250.

16. Y.-D. Yang, K. Iwamoto, E. Tokunaga, N. Shibata, Chem. Commun. 49 (2013) 5510-5512.

17. (a) B. Zhang, A. Studer, Org. Lett. 16 (2014) 1216-1219. (b) Y. Ye, K. P. S. Cheung, L. He, G. C. Tsue, Org. Lett. 20 (2018) 1676-1679.

18. (a) C. K. Prier, D. A. Rankic, D. W. C. Macmillan, Chem. Rev. 113 (2013) 5322-5363; (b) J. M. R. Narayanam, C. R. J. Stephenson, Chem. Soc. Rev. 40 (2011) 102-113; (c) N. A. Romero D. A. Nicewicz, Chem. Rev. 116 (2016) 10075-10166; (d) M. H. Shaw, J. Twilton, D. W. C. Macmillan, J. Org. Chem. 81 (2016) 6898-6926.

19. L. Cui, Y. Matusaki, N. Tada, T. Miura, B. Uno, A. Itoh, Adv. Synth. Catal. 355 (2013) 2203-2207.

20. (a) Q. Lefebvre, N. Hoffmann, M. Rueping, Chem. Commun. 52 (2016) 2493-2496. (b) L. Zhao, P. Li, X. Xie, L. Wang, Org. Chem. Front. 5 (2018) 1689-1697. (c) H.-T. Qin, S.-W. Wu, J.-L. Liu, F. Liu, Chem. Commun. 53 (2017) 1696-1699

21. D. J. Wilger, N. J. Gesmundo, D. A. Nicewicz, Chem. Sci. 4 (2013) 3160-3165.

22. (a) J. F. Berrien, M. Ourévitch, G. Morgant, N. E. Ghermani, B. Crousse, D. Bonnet-Delpon, J. Fluorine Chem. 128 (2007) 839-843; (b) B. Satpathi, S. S. V. Ramasastry, Angew. Chem. Int. Ed. 55 (2016) 1894-1898.

23. T. Yamaguchi, E. Yamaguchi, A. Itoh, Org. Lett. 19 (2017) 1282-1285.

24. (a) T. A. Hamlin, G. M. L. Lazarus, C. B. Kelly, N. E. Leadbeater, Org. Process Res. Dev. 18 (2014) 1253-1258; (b) T. A. Hamlin, C. B. Kelly, R. M. Cywar, N. E. Leadbeater, J. Org. Chem. 79 (2014) 1145-1155. (c) T. A. Hamlin, C. B. Kelly, N. E. Leadbeater, Eur. J. Org. Chem. (2013) 3658-3661; (d) C. B. Kelly, M. A. Mercadante, T. A. Hamlin, M. H. Fletcher, N. E. Leadbeater, J. Org. Chem. 77 (2012) 8131-8141; (e) D. M. Rudzinkski, C. B. Kelly, N. E. Leadbeater, Chem. Commun. 48 (2012) 9610-9612.

25. For key examples, see: (a) J. W. Beatty, J. J. Douglas, K. P. Cole, C. R. J. Stephenson, Nat. Commun. 6 (2015) 7919; (b) D. A. Nagib, D. W. C. MacMillan, Nature 480 (2016) 224-228; (c) J. Jacquet, S. Blanchard, E. Derat, D. E.-L. Murr, L. Fensterbank, Chem. Sci. 7 (2016) 2030-2036.

26. (a) B. Satpathi, S. S. V. Ramasastry, Angew. Chem. Int. Ed. 55 (2016) 1894-1898; (b) B. Elsler, A. Wiebe, D. Schollmeyer, K. M. Dyballa, R. Franke, S. R. Waldvogel, Chem. Eur. J. 21 (2015) 12321-12325; (c) Y.-L. Liu, T.-D. Shi, F. Zhou, X.-L. Zhao, X. Wang, J. Zhou, Org. Lett. 13 (2011) 3826-3829.

27. A. D. Becke, Phys. Rev. A 38 (1988) 3098-3100.

28. J. P. F. Perdew, Phys. Rev. B 33 (1986) 8822-8824.

29. E. van Lenthe, E. J. Baerends, J. Comput. Chem. 24 (2003) 1142-1156.

30. G. te Velde, F. M. Bickelhaupt, E. J. Baerends, C. Fonseca Guerra, S. J. A. van Gisbergen, J. G. Snijders, T. Ziegler, J. Comput. Chem. 22 (2001) 931-967.

31. C. Fonseca Guerra, J. G. Snijders, G. te Velde, E. J. Baerends, Theor. Chem. Acc. 99 (1998) 3910-403.

32. C. C. Pye, T. Ziegler, Theor. Chem. Acc. 101 (1999) 396-408.

33. A. Klamt, G. Schüürmann, J. Chem. Soc. Perkin Trans. 2 (1993) 799-805.

34. A. Klamt, J. Phys. Chem. 99 (1995) 2224-2235.

35. A. Klamt, V. Jonas, J. Chem. Phys. 105 (1996) 9972-9981.

36. Y. Itoh, K. N. Houk, K. Mikami, J. Org. Chem. 71 (2006) 8918-8925.

37. J. M. Sangster, J. C. J. Thynne, J. Phys. Chem. 73 (1969) 2746-2750.

38. J. M. Tedder, J. C. Walton, Adv. Phys. Org. Chem. 16 (1978) 51-86.

39. A. Bottoni, J. Chem. Soc. Perkin Trans. 2 (1996) 2041-2047.

40. J. Korchowiec, T. Uchimaru, J. Phys. Chem. A 102 (1998) 2439-2442.

41. A. P. Stefani, M. Szwarc, A. Kuboyama, S. Matsuzaki, H. Takagi, H. Arano, T. Zytowski, H. Fischer, J. Korchowiec, T. Uchimaru, J. Am. Chem. Soc. 102 (1997) 2439-2442.

42. A. P. Stefani, M. Szwarc, J. Am. Chem. Soc. 84 (1962) 3661-3666.

43. S. Akoka, L. Barantin, M. Trierweiler, Anal. Chem. 71 (1999) 2554-2557.